

1
2
3
4
5
6
7
8
9
10
11
12
13
14
15
16
17
18
19
20
21
22

Amino acid substitutions away from the RNase H catalytic site increase the thermal stability of Moloney murine leukemia virus reverse transcriptase through RNase H inactivation

Atsushi Konishi^a, Tetsuro Hisayoshi^a, Kanta Yokokawa^a, Verónica Barrioluengo^b, Luis Menéndez-Arias^b, Kiyoshi Yasukawa^{a,*}

^a*Division of Food Science and Biotechnology, Graduate School of Agriculture, Kyoto University, Sakyo-ku, Kyoto 606-8502, Japan*

^b*Centro de Biología Molecular “Severo Ochoa” (Consejo Superior de Investigaciones Científicas and Universidad Autónoma de Madrid), c/Nicolás Cabrera 1, Campus de Cantoblanco, 28049 Madrid, Spain*

* Corresponding author. Fax: +81-75-753-6265.
E-mail address: yasukawa@kais.kyoto-u.ac.jp (K. Yasukawa)

Abbreviations: HIV-1, human immunodeficiency virus type 1; MMLV, Moloney murine leukemia virus; RNase H, ribonuclease H; RT, reverse transcriptase; PAGE, polyacrylamide gel electrophoresis

1 **Abstract**

2

3 We have previously used site-directed mutagenesis to introduce basic residues (i.e. Arg;
4 Lys) in the nucleic acid binding cleft of the Moloney murine leukemia virus reverse
5 transcriptase (MMLV RT) in order to increase its template-primer (T/P) binding affinity.
6 Three stabilizing mutations (i.e. E286R, E302K, and L435R) were identified (K.
7 Yasukawa *et al.*, J. Biotechnol., 150 (2010) 299–306). Now, we studied the mechanism
8 by which those mutations increase the thermal stability of the RT. The three
9 single-mutants (E286R, E302K, and L435R), an RNase H-deficient MMLV RT
10 (carrying the RNase H-inactivating mutation D524A), a quadruple mutant
11 (E286R/E302K/L435R/D524A, designated as MM4) and the wild-type enzyme (WT)
12 were produced in *Escherichia coli*. All RTs exhibited similar dissociation constants (K_d)
13 for heteropolymeric DNA/DNA (2.9–6.5 nM) and RNA/DNA complexes (1.2–2.9 nM).
14 Unlike the WT, mutant enzymes (E286R, E302K, L435R, D524A, and MM4) were
15 devoid of RNase H activity, and were not able to degrade RNA in RNA/DNA
16 complexes. These results suggest that the mutations, E286R, E302K, and L435R
17 increase the thermostability of MMLV RT not by increasing its affinity for T/P but by
18 abolishing its RNase H activity.

19

20 *Keywords:* Moloney murine leukemia virus; reverse transcriptase; RNase H activity;
21 template-primer; thermostabilization

1 **1. Introduction**

2
3 Retroviral reverse transcriptase (RT) [EC 2.7.7.49] possesses RNA- and
4 DNA-dependent DNA polymerase as well as RNase H activities. Moloney murine
5 leukemia virus (MMLV) RT is extensively used in cDNA synthesis [1]. MMLV RT is a
6 75-kDa monomer, comprised of the fingers, palm, thumb, and connection subdomains
7 and an RNase H domain [2,3]. The active site of the DNA polymerase activity is located
8 in the palm subdomain while residues in the fingers and thumb subdomains participate
9 in nucleotide and primer binding.

10 Improving the efficiency of the RT DNA polymerase activity at high temperatures
11 has been an important area of research in biotechnology. Available RTs efficient at high
12 temperatures have been obtained by inactivating their RNase H activity [4-8], or by
13 improving template-primer binding affinity [9-11]. Random mutagenesis [12,13] and
14 rational design [9-11] have been used to generate those RT variants. Thermostable RTs
15 from MMLV [4-6], avian myeloblastosis virus (AMV) [5,7], and human
16 immunodeficiency virus type 1 (HIV-1) [8] have been generated by deleting the RNase H
17 H domain [5] or by site-directed mutagenesis of the catalytic residues of the RNase H
18 activity [6-8]. Using random mutagenesis, Arezi and Hogrefe identified five stabilizing
19 mutations of MMLV RT (i.e. E69K, E302R, W313F, L435G, and N454K) [12], and
20 Baranauskas *et al.* indentified another five stabilizing mutations (i.e. L139P, D200N,
21 T330P, L603W, and E607K) [13]. The obtained RTs with mutations
22 E69K/E302R/W313F/L435G/N454K [12] and L139P/D200N/T330P/L603W/E607K
23 [13] exhibited remarkable thermostability. In the case of
24 E69K/E302R/W313F/L435G/N454K, thermostabilization has been attributed to an

1 increase in template-primer (T/P) binding affinity.

2 We have previously identified five stabilizing mutations (E286R, E302K, L435R,
3 V433K, and V433R) [9,10] by introducing basic residues in the nucleic acid binding
4 cleft of the RT. In those studies, we hypothesized that the introduction of positive
5 charges increases the thermostability of MMLV RT by improving its ability to bind the
6 T/P that is negatively charged. Now, we show evidence that reveals that mutations
7 E286R, E302K, and L435R responsible for the higher thermal stability of the RT do not
8 affect T/P binding affinity, but abolish the RNase H activity of the polymerase.

9

10 **2. Materials and methods**

11

12 *2.1. Expression and purification of recombinant MMLV RT*

13

14 Recombinant MMLV RT was prepared as described previously [6]. *Escherichia*
15 *coli* strain BL21(DE3) was transformed with the pET-22b(+) plasmid (Merck
16 Bioscience, Tokyo, Japan) harboring the nucleotides sequence encoding the MMLV RT
17 with a C-terminal (His)₆-tag. *E. coli* cells were harvested from a 2-liter culture, and
18 resuspended in 20 ml of 20 mM potassium phosphate (pH 7.2) buffer, containing 2 mM
19 dithiothreitol (DTT) and 10% (v/v) glycerol (buffer A). After adding 1 mM
20 phenylmethylsulfonyl fluoride (PMSF) to buffer A, cells were sonicated. After
21 centrifugation at 20,000 x g for 40 min, the supernatant was collected and applied to a
22 column [25 mm (inner diameter) x 120 mm] packed with Toyopearl DEAE-650 M gel
23 (Tosoh, Tokyo, Japan), previously equilibrated with buffer A. The column was washed
24 with 80 ml of buffer A containing 120 mM NaCl and eluted with buffer A containing

1 300 mM NaCl, to which saturated $(\text{NH}_4)_2\text{SO}_4$ was added to a final 40% saturation. After
2 centrifugation at 20,000 x g for 30 min, the pellet was collected and dissolved in 10 ml
3 of buffer A containing 500 mM NaCl. After centrifugation at 20,000 x g for 5 min, the
4 supernatant was applied to the column packed with a Ni^{2+} -SephacroseTM (HisTrap HP 1
5 ml, GE Healthcare, Buckinghamshire, UK), previously equilibrated with buffer A. The
6 column was washed with 50 ml of 50 mM Tris-HCl (pH 8.3) buffer, containing 200 mM
7 KCl, 2 mM DTT, 10% glycerol, and 50 mM imidazole, and the RT was eluted with 3 ml
8 of 50 mM Tris-HCl (pH 8.3) buffer, containing 200 mM KCl, 2 mM DTT, 10% glycerol,
9 and 500 mM imidazole. The eluate was then applied to the column packed with a
10 Sephadex G-25 (PD-10, GE Healthcare), previously equilibrated with 50 mM Tris-HCl
11 (pH 8.3), containing 200 mM KCl and 50% glycerol (buffer B). The column was
12 washed and eluted with the same buffer. This sequential chromatography procedures
13 consisting of the Ni^{2+} -SephacroseTM column and the Sephadex G-25 column were
14 repeated two more times. The eluate at the final step was further purified by
15 chromatography on the Sephadex G-25 column. Purified MMLV RT was stored at -80°C
16 before use. MMLV RT concentration was determined using the Protein Assay CBB
17 Solution (Nacalai Tesque, Kyoto, Japan) using bovine serum albumin as standard.

18

19 *2.2. Thermal inactivation of MMLV RT*

20

21 MMLV RT (100 nM) in 10 mM potassium phosphate (pH 7.6) buffer, containing 2
22 mM DTT, 0.2% Triton X-100, and 10% glycerol was incubated in the presence and
23 absence of 28 μM poly(rA)-p(dT)₁₅ at 50°C for 10 min followed by incubation on ice
24 for 30 min. The residual DNA polymerase activity of MMLV RT was measured as

1 described previously [9]. Briefly, the reaction was carried out in 25 mM Tris-HCl (pH
2 8.3) buffer, containing 50 mM KCl, 2 mM DTT, 5 mM MgCl₂, 25 μM poly(rA)-p(dT)₁₅
3 (this concentration is expressed as that of p(dT)₁₅), 0.2 mM [³H]dTTP, and 10 nM
4 MMLV RT at 37°C. Aliquots of 20 μl were collected at different times and immediately
5 spotted onto glass microfiber filters GF/C of 2.5 cm (Whatman, Middlesex, UK).
6 Unincorporated [³H]dTTP was removed by three washes with chilled 5% (w/v)
7 trichloroacetic acid for 10 min each followed by one wash with chilled 95% ethanol.
8 The amounts of [³H]dTTP incorporated were determined by scintillation counting in 2.5
9 ml of Ecoscint H solution (National Diagnostics, Atlanta, GA) using a LSC-5100
10 apparatus (Aloka, Mitaka, Japan), and the initial reaction rate was determined.

11

12 *2.3. Determination of dissociation constants (K_d) of RT-T/P complex*

13

14 The 31T(DNA) or the 31T (RNA) and the 21P-C(DNA) labelled with [γ -³²P]ATP
15 (PerkinElmer, Boston, MA) at its 5'-terminus were annealed to generate T/Ps
16 31T(DNA)/[³²P]21P-C(DNA) and 31T(RNA)/[³²P]21P-C(DNA). MMLV RTs (12 nM)
17 were pre-incubated with various concentrations of either of the two duplexes (2-40 nM)
18 at 37°C for 10 min in 20 μl of 50 mM Tris-HCl (pH 8.0) buffer, containing 50 mM KCl.
19 Reactions were initiated by adding 20 μl of 50 mM Tris-HCl (pH 8.0) buffer, containing
20 20 mM dTTP, 50 mM KCl, 30 mM MgCl₂, and 20 μM 31T(DNA)/21P-C(DNA). The
21 31T(DNA)/21P-C(DNA) at high concentration (20 μM) binds unbound RT as well as
22 RT that dissociates from DNA/DNA or RNA/DNA duplexes, preventing further RT
23 binding to labelled T/Ps. Aliquots of 4 μl were removed at 15, 30, and 45 s, and

1 immediately quenched with 4 μ l of sample-loading buffer (10 mM EDTA, 90% (v/v)
2 formamide, 3 mg/ml xylene cyanol FF, 3 mg/ml bromophenol blue, and 50 μ M
3 31T(DNA)/21P-C(DNA)). The reaction products were analyzed by denaturing 20%
4 polyacrylamide gel electrophoresis and quantified with a BAS-2500 scanner (Fujifilm,
5 Tokyo, Japan) using the program Multi Gauge version 2.2 (Fujifilm). For each reaction,
6 the percentage of elongated primer was plotted against the incubation times and the data
7 were fit to a linear equation. As the concentration of template-primer is well above the
8 dissociation constant of MMLV RT, K_d , under this assay conditions, the RT-T/P
9 concentration, [RT-T/P], in the preincubated mixture was calculated from the y-intercept
10 that represents the amount of RT bound to template-primer at time zero. The K_d values
11 were determined by fitting the data thus obtained to Eq. 1.

12

$$13 \quad [RT-T/P] = 0.5 \times (K_d + [RT]_o + [T/P]_o) - 0.5 \times \{(K_d + [RT]_o + [T/P]_o)^2 - 4[RT]_o[T/P]_o\}^{0.5} \quad (1)$$

14

15 where K_d is the dissociation constant of MMLV RT with T/P, and $[RT]_o$ and $[T/P]_o$ is the
16 initial RT and T/P concentration, respectively, in the preincubated mixture. The relative
17 RT-T/P concentration, defined as the ratio of the respective RT-T/P concentration to the
18 maximum values obtained, was plotted as a function of the initial T/P concentration.

19

20 *2.4. Extension of primers in the absence of one dNTP.*

21

22 The DNA polymerase activity of MMLV RT in the absence of one dNTP was
23 determined using a method previously described [14]. Briefly, the reaction (40 μ l) was
24 carried out at 37°C in 50 mM Tris-HCl (pH 8.0) buffer, containing 50 mM KCl, 15 mM

1 MgCl₂, 150 nM MMLV RT, 20 nM D2-47(DNA)/[³²P]PG5-25(DNA), and 250 μM each
2 dNTP. The reaction was stopped after a two-hour incubation, and the reaction products
3 were analyzed as described above (section 2.3).

4 5 2.5. RNase H activity assay

6
7 The RNase H activity of MMLV RT was determined as described previously [15].
8 Briefly, four RNA/DNA duplexes were prepared. The reaction (40 μl) was carried out in
9 50 mM Tris-HCl (pH 8.0) buffer, containing 50 mM KCl, 15 mM MgCl₂, 150 nM
10 MMLV RT, and 20 nM [³²P]31T(RNA)/21P-C(DNA), [³²P]D2-47(RNA)/PG5-25(DNA),
11 [³²P]D2-25(RNA)/PG5-25(DNA), or [³²P]31T(RNA)/15P(DNA) at 37°C for 0-40 min.
12 Then aliquots were removed at different times (0.25, 0.5, 2, 4, 20, and 40 min), and
13 reaction products were analyzed as described above (section 2.3).

14 15 3. Results

16 17 3.1. Preparation and characterization of MMLV RT

18 We previously generated four thermostable MMLV RT variants by introducing
19 single amino acid substitutions (E286R, E302K, L435R, and D524A) as well as one
20 quadruple variant (E286R/E302K/L435R/D524A, designated as MM4) [9]. Wild-type
21 enzyme (WT) and all mutant RTs were expressed in *E. coli* and purified to homogeneity.
22 RTs were judged to be pure by SDS-PAGE, and the *M_r* values obtained were around
23 75,000 (Fig. 1A).

24 DNA polymerase activities of all enzymes were determined at 37°C after

1 incubation at 50°C for 10 min in the presence and absence of T/P (Fig. 1B). Each
2 enzyme exhibited higher relative activity in the presence of T/P than in its absence, and
3 all variants exhibited higher relative activities than WT both in the presence and the
4 absence of T/P. These results are in agreement with those published in our previous
5 report [9].

6 We measured UV, CD, and fluorescence spectra of the purified enzymes. All
7 enzymes exhibited similar UV spectra with maximum absorbance at 275 nm (Fig. S1A).
8 On CD spectroscopy, all RTs exhibited negative ellipticities at around 202–250 nm with
9 minimum values around 208 and 222 nm (Fig. S1B). At excitation wavelength of 280
10 and 295 nm, all RTs exhibited emission fluorescence spectra with maximum intensities
11 at 338 nm (Fig. S1C). No appreciable changes were observed in each spectra between
12 WT and variants.

13

14 *3.2. Effect of stabilizing mutations on the affinities of MMLV RT for T/P*

15 In order to test whether individual mutations such as E286R, E302K, and L435R
16 would affect T/P binding affinity, we determined the dissociation constants (K_d) of
17 RT-T/P complexes. RTs were pre-incubated with various concentrations of radiolabelled
18 T/P to form an RT-T/P complex. The reaction was initiated by adding dTTP, Mg^{2+} , and
19 an excess of unlabelled T/P, and the products were analyzed. Figure 2 shows the relative
20 concentration of the RT-T/P complex *versus* the total T/P concentration in the
21 preincubated mixture. Saturation curves were obtained for DNA/DNA (Fig. 2A) and
22 RNA/DNA (Fig. 2B) duplexes. The K_d values obtained with the DNA/DNA duplex and
23 RTs WT, E286R, E302K, L435R, D524A, and MM4 were 2.9 ± 0.3 , 3.5 ± 0.6 , 6.5 ± 1.2 ,
24 5.4 ± 0.5 , 3.3 ± 0.4 , and 2.9 ± 0.3 nM, respectively, and the values obtained with the

1 RNA/DNA duplex were 2.0 ± 0.3 , 1.7 ± 0.2 , 2.9 ± 0.3 , 2.7 ± 0.4 , 2.6 ± 0.2 , and 1.2 ± 0.2 nM,
2 respectively. These data indicate that WT and mutant RTs have similar binding affinities
3 for T/P. The results also show that the binding affinities of MMLV RTs for the
4 RNA/DNA duplex (K_d values of 1.2–2.9 nM) are slightly higher than for the DNA/DNA
5 duplex (2.9–6.5 nM).

6

7 *3.3. Effect of the stabilizing mutations on the fidelities of MMLV RT*

8 The effects of stabilizing mutations on the fidelity of MMLV RT were determined
9 by measuring primer extension in the absence of one dNTP (Fig. 3). In the presence of
10 all four dNTPs, fully-extended products of 47-nucleotides (nt) were obtained with all
11 enzymes. In the absence of dGTP, the same result was obtained, compatible with the
12 sequence of D2-47/PG5-25 in which dGTP is not required for faithful extension. When
13 dATP was absent, in WT, E286R, L435R, and D524A, the intensities of the bands
14 corresponding to 42- and 43-nt products were similar, while in reactions carried out
15 with mutants E302K and MM4, the intensity of the 42-nt band was stronger than the
16 intensity of the 43-nt band. This result is consistent with a lower misincorporation of A
17 at position 43, by mutant E302K, suggesting that this mutation increases the fidelity of
18 MMLV RT, while E286R, L435R, and D524A do not.

19

20 *3.4. Effect of the stabilizing mutations on the RNase H activities of MMLV RT*

21 It is known that the loss of RNase H activity caused by the mutation of the
22 catalytic residue, Asp524, increases the stability of the RNA in reverse transcription
23 reactions and improves the efficiency of the DNA polymerase activity [5]. In order to
24 determine whether the three stabilizing mutations affect the RNase H activity, we

1 measured the RNase H activities of WT and mutant enzymes with the RNA/DNA
2 hybrid, [³²P]31T(RNA)/21P-C(DNA), consisting of 31-nt RNA and 21-nt DNA as the
3 substrate (Fig. 4A). In reactions carried out with WT RT, evidence of cleavage was
4 demonstrated by the presence of RNA bands of 28-nt or smaller, indicating that the
5 RNA strand of the hybrid was first cleaved at the position of 18-bp upstream of the
6 primer 3'-terminus. As expected, in D524A and MM4 of which the catalytic residue for
7 RNase H activity, Asp524, is mutated to Ala, RNA remained undegraded. Unexpectedly,
8 the mutants E286R, E302K, and L435R did not show RNase H activity, and RNA
9 templates remained uncleaved after 40-min incubation at 37°C (Fig. 4A).

10 In reactions carried out with HIV-1 RT, the RNA strand of an RNA/DNA hybrid is
11 cleaved at the position of 16-bp upstream of the primer 3'-terminus [16], and that such
12 T/P binds HIV-1 RT at its both DNA polymerase and RNase H active sites [17],
13 suggesting that the RNase H activity of MMLV RT varies depending on RNA/DNA
14 hybrid species. To address this possibility, we used three additional RNA/DNA hybrids
15 ([³²P]D2-47(RNA)/PG5-25(DNA) (Fig. 4B), [³²P]D2-25(RNA)/PG5-25(DNA) (Fig.
16 4C), and [³²P]31T(RNA)/15P(DNA)) (Fig. 4D). Each T/P was designed to bind to both
17 the DNA polymerase and RNase H active sites simultaneously, to bind only the RNase
18 H active site due to the lack of primer 3'-terminus, and to bind either of the two active
19 sites but not both simultaneously due to the usage of a shorter primer, respectively. With
20 all RNA/DNA hybrid species, RNAs remained uncleaved in reactions catalyzed by all
21 mutant RTs. This clearly indicates that mutations E286R, E302K, and L435R abrogate
22 the RNase H activity.

23

24 **4. Discussion**

1

2 In this study, we demonstrate that the three stabilizing mutations (E286R, E302K,
3 and L435R) eliminate the RNase H activity of MMLV RT. The crystal structure of the
4 full-length enzyme has not been determined. Crystal structures of the polymerase
5 domains of MMLV RT and the closely related xenotropic murine leukemia virus-related
6 virus (XMRV) RT have been partially determined [2, 18]. These structures reveal the
7 common fold consisting of fingers, palm, thumb, and connection subdomains found in
8 HIV-1 RT. On the other hand, the structures of the isolated RNase H domains of the
9 MMLV RT and XMRV RT have also been determined [19,20]. Molecular models of
10 MMLV RT suggest that the RNase H domain of MMLV RT is positioned far from the
11 fingers/palm/thumb subdomain, like in the structure of the p66 subunit of HIV-1 RT
12 [2,3]. Based on those models, it has been suggested that the RNase H domain alters the
13 trajectory of the T/P, affecting the DNA polymerase activity [2,3]. Moreover, it has been
14 reported that the DNA polymerase activity of a MMLV RT variant lacking the RNase H
15 domain was considerably reduced [21].

16 Amino acid sequence identity between MMLV and XMRV RTs is around 95% [22].
17 The structure of the polymerase domain of XMRV RT bound to an RNA/DNA complex
18 [18] reveals that Glu302 interacts with the T/P, but Glu286 and Leu435 are away from
19 the nucleic acid binding cleft and long-distance effects appear to be responsible for the
20 lack of RNase H activity of the corresponding mutants (Fig. S2).

21 In addition, the results of fidelity assays show that mutations that increase the
22 thermal stability of the MMLV RT have a relatively minor effect on the accuracy of the
23 polymerase. Among the studied mutations, only E302K produced a very modest
24 improvement in the fidelity of the enzyme, detected only at selected sites in primer

1 extension assays carried out in the absence of one nucleotide (Fig. 3).

2 In our study, all variants lacked RNase H activity, as demonstrated using four
3 different RNA/DNA substrates. Two of them were designed with a template overhang to
4 cover the DNA polymerase and the RNase H active sites simultaneously (Fig. 4A and
5 B), a third substrate lacks the overhang and would bind only to the RNase H active site
6 (Fig. 4C), while the fourth one is expected to bind any of the two active sites, but not
7 both simultaneously, due to the relatively short distance between the 3' end of the DNA
8 primer and the putative RNase H cleavage site (Fig. 4D).

9 Taking into account the structures of those substrates, we suggest that the three
10 stabilizing mutations would alter the trajectory of the T/P and prevent its proper binding
11 at the RNase H active site, leading to the loss of the RNase H activity. This is in contrast
12 to the case with the mutation of the catalytic residue for the RNase H activity, Asp524.
13 In this case, the RNase H active site cannot bind Mg^{2+} , leading to the loss of RNase H
14 activity. In addition, it should be mentioned that the rate of the degradation reaction
15 observed with the WT RT and the substrate [^{32}P]D2-25(RNA)/PG5-25(DNA) (Fig. 4C)
16 is similar to rates calculated from assays shown in Figs. 4A and B, suggesting the
17 possibility that the substrate used in Fig. 4C binds both the DNA polymerase and RNase
18 H active sites simultaneously.

19 In this study, we also suggest that the three stabilizing mutations increase the
20 thermostability of MMLV RT not by increasing its affinity for the T/P but by abolishing
21 its RNase H activity. Although it has been reported that the thermostabilities of MMLV,
22 AMV, and HIV-1 RTs are improved by the loss of the RNase H activity through the
23 elimination of the RNase H activity [4-8], the mechanism is unknown. Goedken and
24 Marqusee reported that in the CD analysis of the reversible unfolding of the isolated

1 RNase H domain of MMLV RT (Pro515-Leu671), the midpoint denaturation
2 temperature of D524N was higher by 10°C than that of the WT RT, suggesting that the
3 substitution of Asp524 eliminates the RT's RNase H activity, leading to an increase in
4 the enzyme's intrinsic thermostability as a result of a structural change [23]. In the cases
5 of E286R, E302K, and L435R, it was first thought that the observed higher
6 thermostability was due to the increase in the T/P binding affinity [9]. However, this has
7 been challenged by our data showing that WT and mutant RTs exhibit similar K_d values
8 (Fig. 2). As in the case of D524A, amino acids changes E286R, E302K, and L435R
9 increase the RT's intrinsic thermal stability. Those mutations outside the RNase H
10 catalytic site abolish the RNase H activity of the enzyme but do not affect its affinity for
11 T/P.

12

13 **Acknowledgments**

14

15 This study was supported in part by Grants-in-Aid for Scientific Research (No.
16 21580110 to K. Y.) and for JSPS Fellows (No. 25-1955 to A. K.) from the Japan
17 Society for the Promotion of Science (JSPS). Work in Madrid has been partially
18 supported by Spanish Government grants BIO2010-15542 and BIO2013-48788-C2-1-R.
19 L. M.-A. was recipient of an invitation short-term fellowship of the JSPS (FY2012).

20

21 **References**

22

23 [1] A.R. Kimmel, S.L. Berger, Preparation of cDNA and the generation of cDNA
24 libraries: overview, *Methods Enzymol.*, 152 (1987) 307–316.

- 1 [2] D. Das, M.M. Georgiadis, The crystal structure of the monomeric reverse
2 transcriptase from Moloney murine leukemia virus, *Structure*, 12 (2004)
3 819–829.
- 4 [3] M.L. Coté, M.J. Roth, Murine leukemia virus reverse transcriptase: structural
5 comparison with HIV-1 reverse transcriptase. *Virus Res.*, 134 (2008) 186–202.
- 6 [4] M.L. Kotewicz, J.M. D'Alessio, K.M. Driftmier, K.P. Blodgett, G.F. Gerard,
7 Cloning and overexpression of Moloney murine leukemia virus reverse
8 transcriptase in *Escherichia coli*, *Gene*, 35 (1985) 249–258.
- 9 [5] G.F. Gerard, R.J. Potter, M.D. Smith, K. Rosenthal, G. Dhariwal, J. Lee, D.K.
10 Chatterjee, The role of template-primer in protection of reverse transcriptase from
11 thermal inactivation, *Nucleic Acids Res.*, 30 (2002) 3118–3129.
- 12 [6] M. Mizuno, K. Yasukawa, K. Inouye, Insight into the mechanism of the
13 stabilization of Moloney murine leukaemia virus reverse transcriptase by
14 eliminating RNase H activity, *Biosci. Biotechnol. Biochem.*, 74 (2010) 440–442.
- 15 [7] A. Konishi, K. Yasukawa, K. Inouye, Improving the thermal stability of avian
16 myeloblastosis virus reverse transcriptase α -subunit by site-directed mutagenesis,
17 *Biotechnol. Lett.*, 34 (2012) 1209–1215.
- 18 [8] K. Nishimura, M. Shinomura, A. Konishi, K. Yasukawa, Stabilization of human
19 immunodeficiency virus type 1 reverse transcriptase by site-directed mutagenesis,
20 *Biotechnol. Lett.*, 35 (2013) 2165–2175.
- 21 [9] K. Yasukawa, M. Mizuno, A. Konishi, K. Inouye, Increase in thermal stability of
22 Moloney murine leukaemia virus reverse transcriptase by site-directed
23 mutagenesis, *J. Biotechnol.*, 150 (2010) 299–306.
- 24 [10] A. Konishi, X. Ma, K. Yasukawa, Stabilization of Moloney murine leukemia

- 1 virus reverse transcriptase by site-directed mutagenesis of the surface residue
2 Val433, *Biosci. Biotechnol. Biochem.*, 78 (2014) 75–78.
- 3 [11] T. Matamoros, V. Barrioluengo, D. Abia, L. Menéndez-Arias, Major groove
4 binding track residues of the connection subdomain of human immunodeficiency
5 virus type 1 reverse transcriptase enhance cDNA synthesis at high temperatures,
6 *Biochemistry*, 52 (2013) 9318–9328.
- 7 [12] B. Arezi, H. Hogrefe, Novel mutations in Moloney murine leukemia virus reverse
8 transcriptase increase thermostability through tighter binding to template-primer,
9 *Nucleic Acids Res.*, 37 (2009) 473–481.
- 10 [13] A. Baranauskas, S. Paliksa, G. Alzbutas, M. Vaitkevicius, J. Lubiene, V.
11 Letukiene, S. Burinskas, G. Sasnauskas, R. Skirgaila, Generation and
12 characterization of new highly thermostable and processive M-MuLV reverse
13 transcriptase variants, *Protein Eng. Des. Sel.*, 25 (2012) 657–668.
- 14 [14] M. Gutiérrez-Rivas, Á. Ibáñez, M.A. Martínez, E. Domingo, L. Menéndez-Arias,
15 Mutational analysis of Phe160 within the “palm” subdomain of human
16 immunodeficiency virus type 1 reverse transcriptase, *J. Mol. Biol.*, 290 (1999)
17 615–625.
- 18 [15] M. Álvarez, T. Matamoros, L. Menéndez-Arias, Increased thermostability and
19 fidelity of DNA synthesis of wild-type and mutant HIV-1 group O reverse
20 transcriptases, *J. Mol. Biol.*, 392 (2009) 872–884.
- 21 [16] G. Betancor, M.C. Puertas, M. Nevot, C. Garriga, M.A. Martínez, J.
22 Martinez-Picado, L. Menéndez-Arias, Mechanisms involved in the selection of
23 HIV-1 reverse transcriptase thumb subdomain polymorphisms associated with
24 nucleoside analogue therapy failure, *Antimicrob. Agents Chemother.*, 54 (2010)

- 1 4799–4811.
- 2 [17] G.L. Beilhartz, M. Wendeler, N. Baichoo, J. Rausch, S. Le Grice, M. Götte,
3 HIV-1 reverse transcriptase can simultaneously engage its DNA/RNA substrate at
4 both DNA polymerase and RNase H active sites: implications for RNase H
5 inhibition, *J. Mol. Biol.*, 388 (2009) 462–474.
- 6 [18] E. Nowak, W. Potrzebowski, P.V. Konarev, J.W. Rausch, M.K. Bona, D.I.
7 Svergun, J.M. Bujnicki, S.F.J. Le Grice, M. Nowotny, Structural analysis of
8 monomeric retroviral reverse transcriptase in complex with an RNA/DNA hybrid,
9 *Nucleic Acid Res.*, 41 (2013) 3874–3887.
- 10 [19] D. Lim, G.G. Gregorio, C. Bingman, E. Martinez-Hackert, W.A. Hendrickson,
11 S.P. Goff, Crystal structure of the Moloney murine leukemia virus RNase H
12 domain, *J. Virol.*, 80 (2006) 8379–8389.
- 13 [20] D. Zhou, S. Chung, M. Miller, S.F.J. Le Grice, A. Wlodawer, Crystal structures of
14 the reverse transcriptase-associated ribonuclease H domain of *Xenotropic murine*
15 *leukemia-virus related virus*, *J. Struct. Biol.*, 177 (2012) 638–645.
- 16 [21] A. Telesnitsky, S.P. Goff, RNase H domain mutations affect the interaction
17 between Moloney murine leukemia virus reverse transcriptase and its
18 primer-template, *Proc. Natl. Acad. Sci. USA*, 329 (1993) 1276–1280.
- 19 [22] V. Barrioluengo, Y. Wang, S.F.J. Le Grice, L. Menéndez-Arias, Intrinsic DNA
20 synthesis fidelity of xenotropic murine leukemia virus-related virus reverse
21 transcriptase, *FEBS J.*, 279 (2012) 1433–1444.
- 22 [23] E.R. Goedken, S. Marqusee, Metal binding and activation of the ribonuclease H
23 domain from Moloney murine leukemia virus, *Protein Eng.*, 12 (1999) 975–980.

24

1 **Figure legends**

2

3 **Fig. 1. Purification and characterization of MMLV RT.** (A) SDS-PAGE under
4 reducing conditions. Enzyme (1.2 μ g) was applied to each lane. Coomassie Brilliant
5 Blue-stained 10% SDS-polyacrylamide gels is shown. (B) Thermal inactivation of
6 MMLV RT. Enzyme was incubated at 50°C for 10 min in the presence (black bar) and
7 the absence (white bar) of poly(rA)-p(dT)₁₅. Then, the dTTP incorporation reaction
8 using poly(rA)-p(dT)₁₅ as T/P was carried out at 37°C. The relative activity was defined
9 as the ratio of the initial reaction rate with heat treatment to that without it. Represented
10 values were obtained from at least three independent experiments.

11

12 **Fig. 2. Dissociation equilibrium of WT and mutant RTs with DNA/DNA and**
13 **RNA/DNA complexes.** WT and mutant RTs were preincubated with various
14 concentrations of 31T(DNA)/[³²P]21P-C(DNA) (A) or 31T(RNA)/[³²P]21P-C(DNA)
15 (B) at 37°C for 10 min. DNA polymerization reactions were initiated by adding dTTP and
16 unlabelled 31T(DNA)/21P-C(DNA). The initial concentrations of RT, dTTP, and
17 unlabelled 31T(DNA)/21P-C(DNA) in the reaction were 6 nM, 10 mM, and 40 μ M,
18 respectively. The solid line is the best fit of the data to Eq. 1. The asterisk indicates the
19 labelled nucleotide with [γ -³²P]ATP. Symbols: WT, open circle; E286R, open triangle;
20 E302K, open square; L435R, open diamond; D524A, closed circle; and MM4, closed
21 triangle.

22

23 **Fig. 3. Primer extension in the absence of one nucleotide.** Reactions were carried out
24 at 37°C for 2 h with 150 nM MMLV RT, 20 nM D2-47(DNA)/[³²P]PG5-25(DNA), and

1 250 μ M each dNTP. Lanes marked with + indicate that all four nucleotides were
2 included in the dNTP mix. The lanes marked with -C, -G, -T, and -A indicate that three
3 nucleotides except dCTP, dGTP, dTTP, or dATP, respectively. Specific bands
4 corresponding to products of 42- and 43-nucleotides are indicated.

5

6 **Fig. 4. RNase H activity.** Reactions were carried out at 37°C for 0-40 min in the
7 presence of 20 nM labelled T/P and 0 or 150 nM RT. The arrows indicate the cleavage
8 sites. Labelled T/P: A, [³²P]31T(RNA)/21P-C(DNA); B,
9 [³²P]D2-47(RNA)/PG5-25(DNA); C, [³²P]D2-25(RNA)/PG5-25(DNA); D,
10 [³²P]31T(RNA)/15P(DNA). The asterisk indicates the position of the ³²P label. Time
11 points were 0.25, 0.50, 2.0, 4.0, 20, and 40 min for WT and 0.25 and 40 min for mutant
12 RTs.

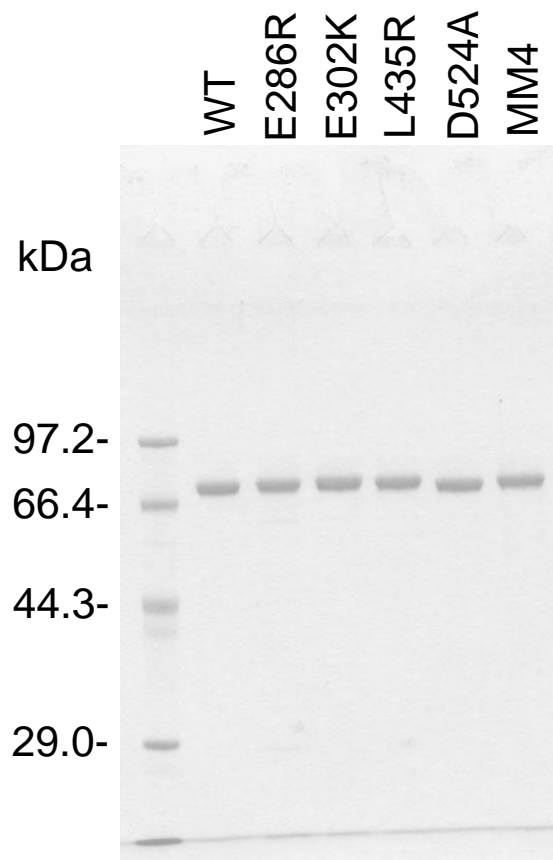
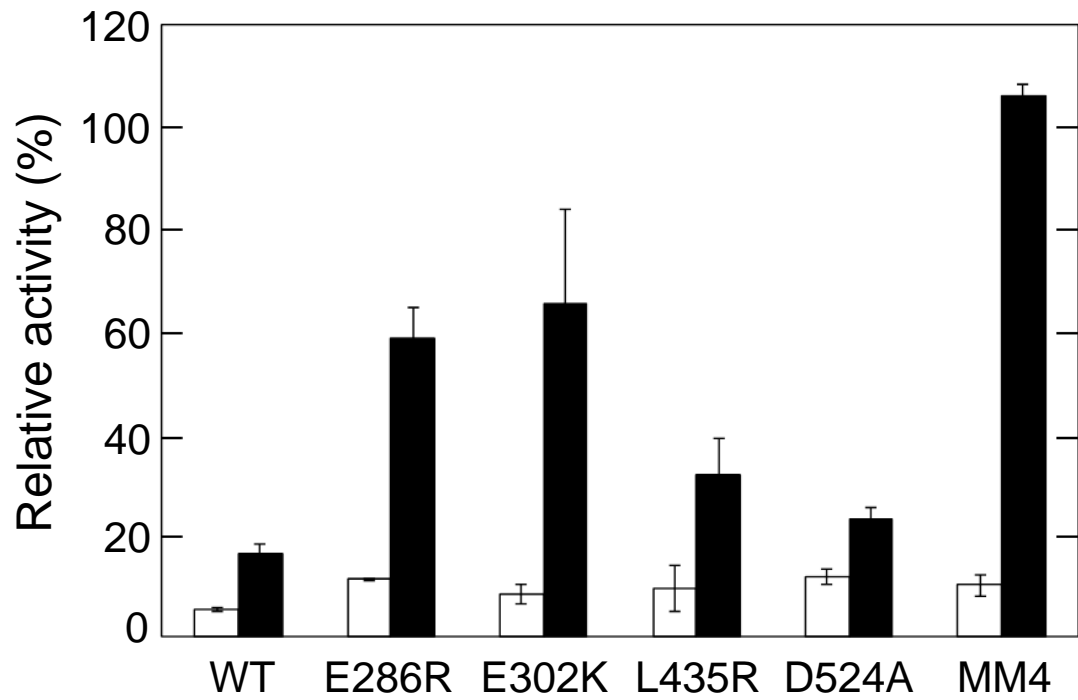
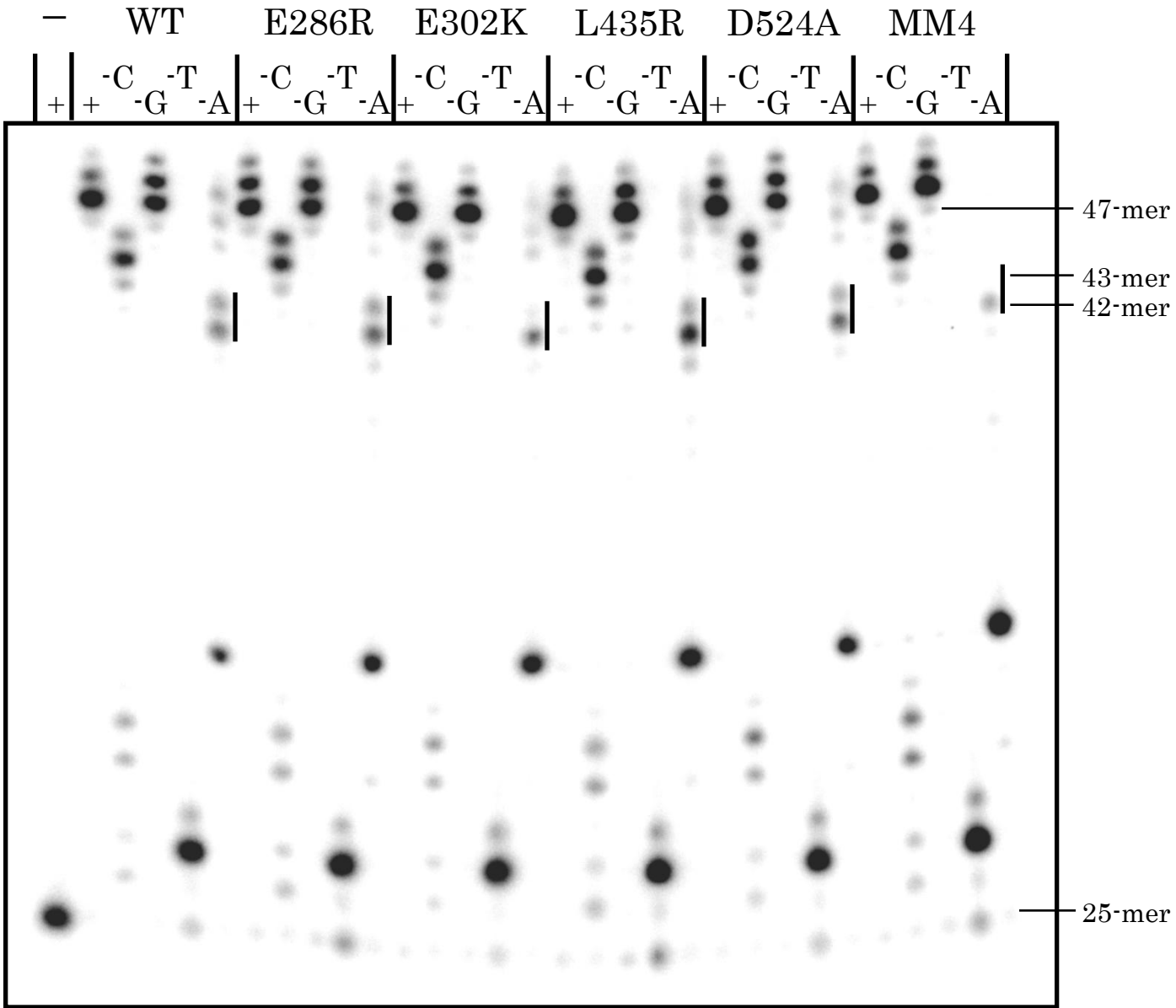
A**B**

Fig. 1, Konishi *et al.*



D2-47 (DNA) : 5'-GGGATTA⁴⁰AAAATAGTA³⁰AAGAATGTATAGCCCTACCAGCATTCTGG-3'
 [32P]PG5-25 (DNA) : 3'-TACATATCGGGATGGTCGTAAGACC*-5'

Fig. 3, Konishi *et al.*

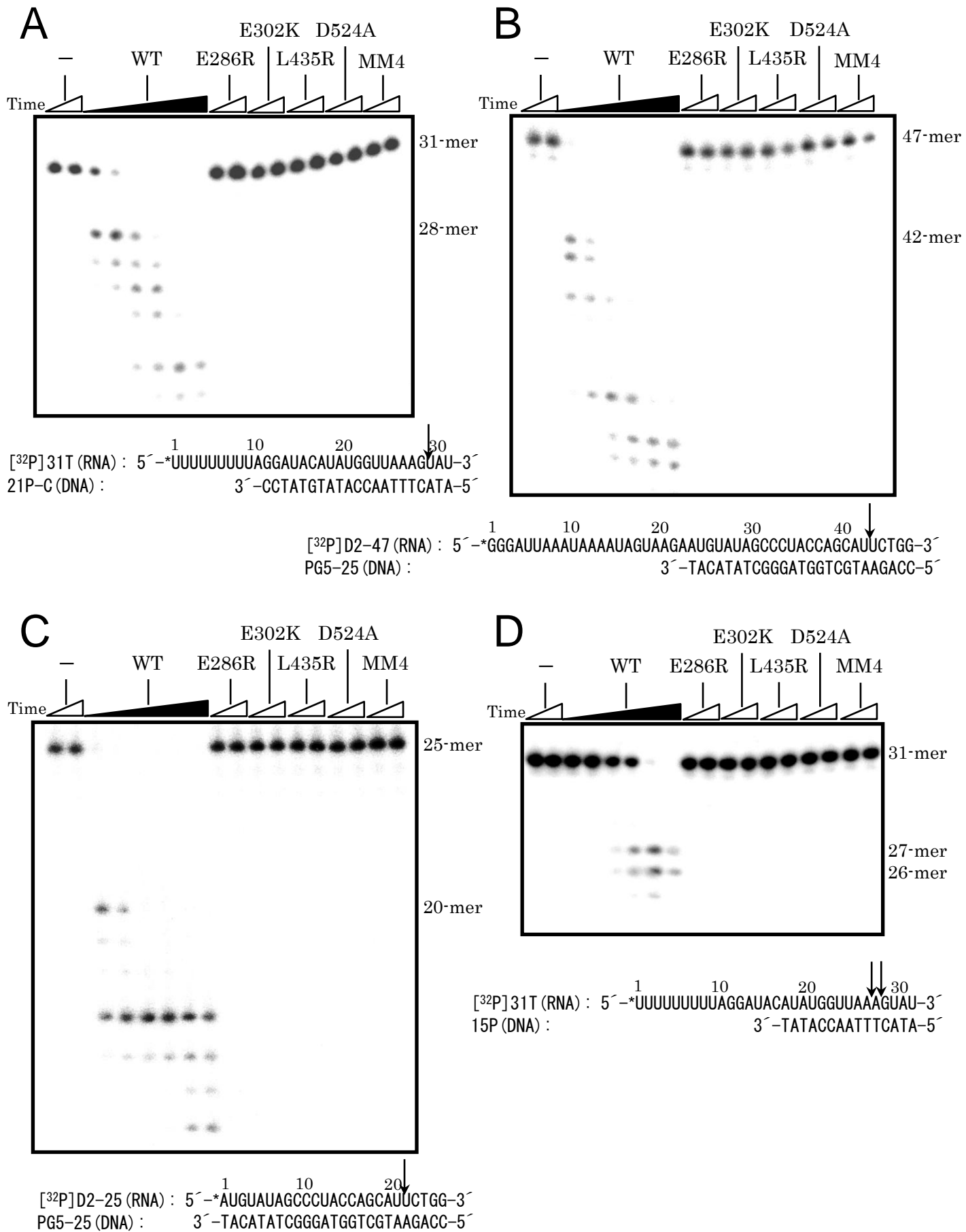
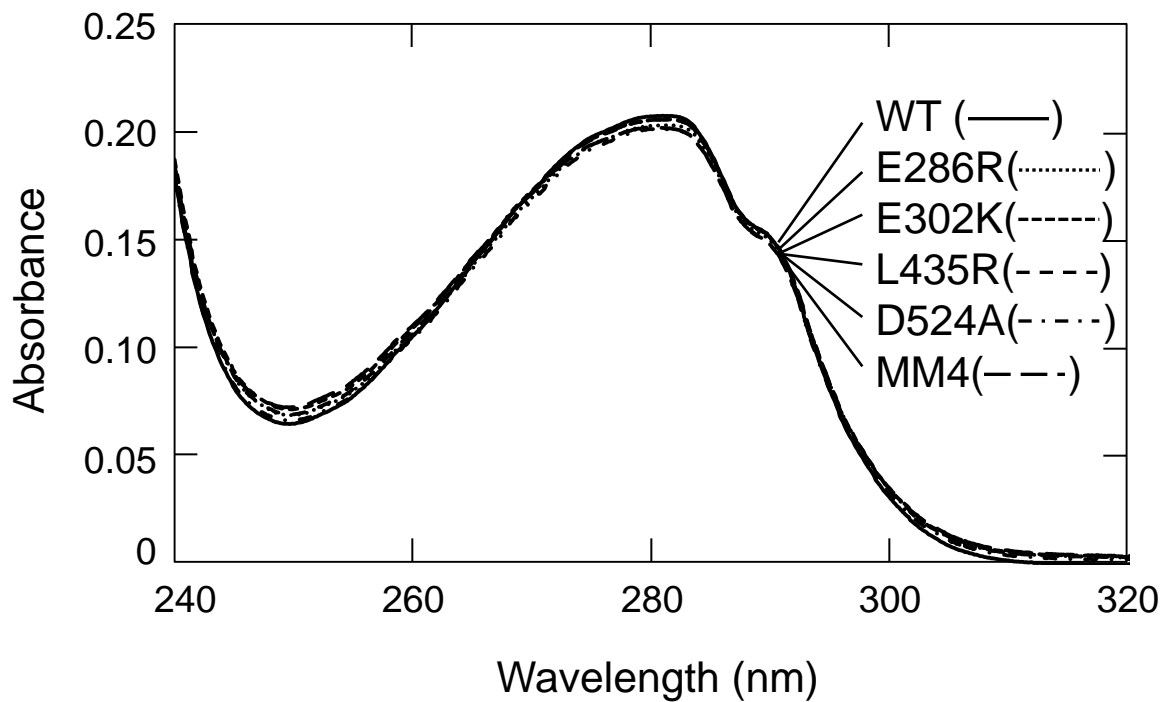
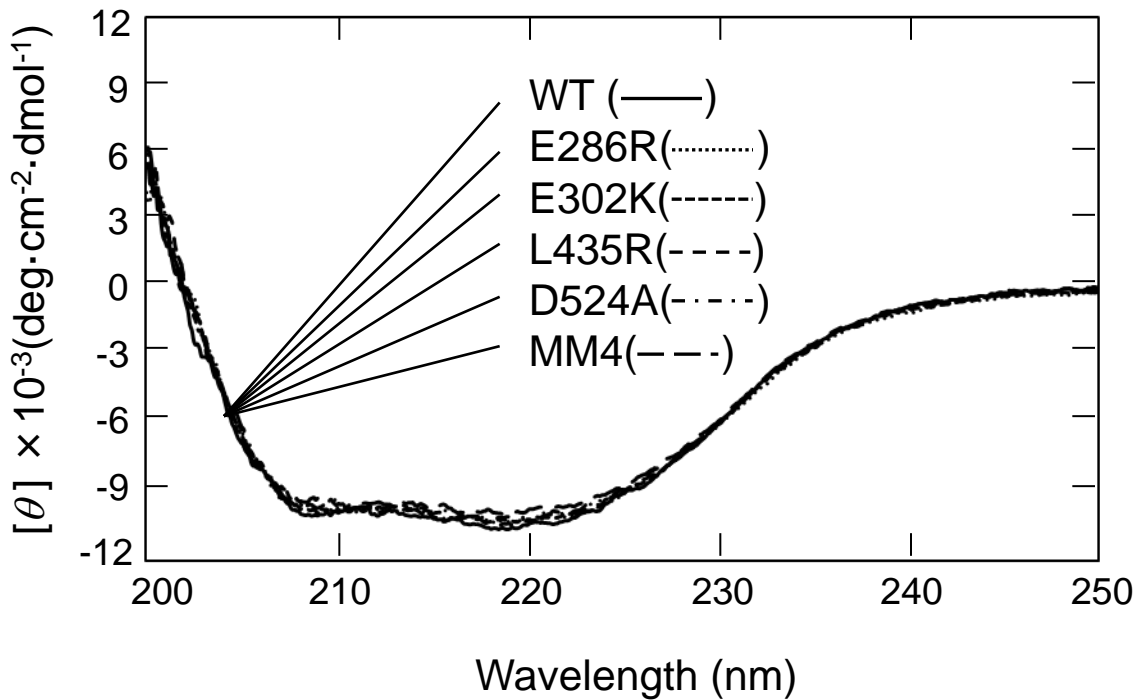


Fig. 4, Konishi *et al.*

A**B**

C

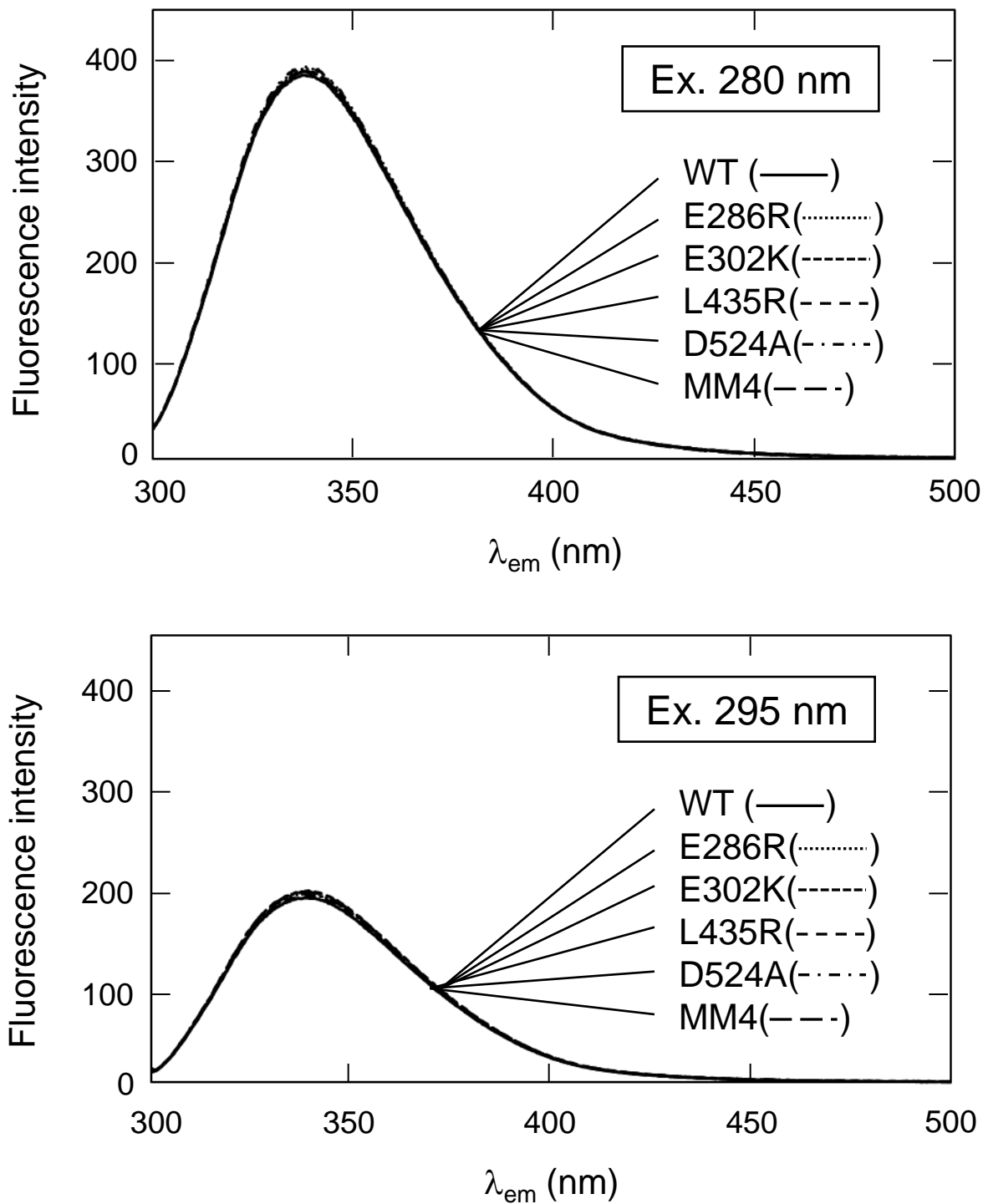


Fig. S1. UV, CD, and fluorescence spectra of MMLV RT. (A) UV spectra. (B) CD spectra. (C) Fluorescence spectra. Spectra were obtained in 50 mM Tris-HCl (pH 8.3) buffer, containing 200 mM KCl and 50% (v/v) glycerol at 25°C with protein concentration of 0.15 mg/ml (A, B) or 0.075 mg/ml (C).

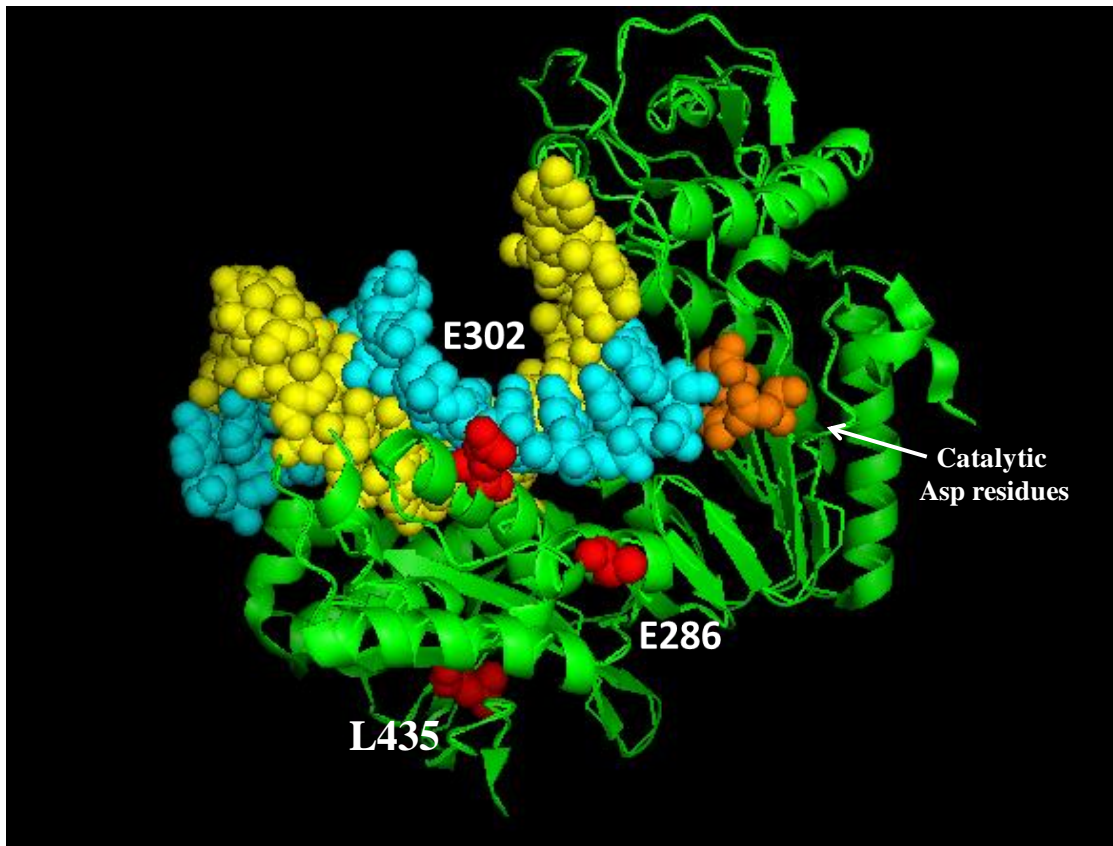


Fig. S2. Location of relevant residues in the crystal structure of the polymerase domain of XMRV RT. The RT backbone is represented with a green cartoon, the RNA/DNA template-primer is shown with spheres (yellow and cyan). Catalytic aspartic acid residues (positions 150, 225, and 226) are shown with orange spheres. Residues equivalent to those replaced in the MMLV RT are indicated in red (i.e. Glu286, Glu302, and Leu435). Coordinates were taken from Protein Data Bank file 4HKQ and the structure was drawn using the PyMol molecular software (<http://www.pymol.org>).